About the Limiting Behaviour of Iterated Robust Morphological Operators

Johan Van Horebeek[1]
Ernesto Tapia-Rodriguez[1 2]

[1] Centro de Investigación en Matemáticas
Ap. Postal 402, 36000 Guanajuato, Gto., Mexico
horebeek@cimat.mx
[2] Freie Universität Berlin, Institut für Informatik
Tacostr. 9, D-14195 Berlin, Germany
tapia@inf.fu-berlin.de

Abstract. We study the limiting behaviour of the repeated application of a discrete image operator that belongs to a recently introduced class of morphological operators. To this purpose, we describe the implied iterative process by a discrete dynamical system.
The convergence is derived for binary and gray scale images.

1 Introduction

Mathematical morphology is an important branch of non-linear signal processing. It has its roots in discrete geometry and set theory, using as a starting point the probing of an image by a small(er) structural element. We refer to [3], [6] and [7] for an overview.

This geometric foundation often facilitates an intuitive interpretation of morphological operators in terms of geometric concepts and is also extremely useful for the derivation of many fundamental properties.

Despite the vast amount of literature about mathematical morphology, the limiting behaviour of the repeated applications of a morphological operator has not received a lot of attention. Partly, this is because in many cases it is a trivial problem: a large class of operators are idempotent (e.g., openings, closings) or decreasing (increasing) functions with a natural lower (resp. upper) bound (e.g., erosions, dilations, openings by reconstruction). This papers aims to make a contribution for non-trivial cases.

The organization is as follows: in section 2, we describe the class of morphological operators, previously introduced in [11], and for which we prove the convergence in section 3. Section 4 explains how the results can be extended to other morphological operators.

In what follows, X will denote a discrete image defined on a finite rectangular grid; X_x returns the gray level value at position x. In the case of a binary image, in order to simplify the notation, X denotes also the set of black pixels, depending on the context. The cardinality of a set S is given by $|S|$; the translation of S

by t, $\{s+t, s \in S\}$ is denoted by $S_{(t)}$ and the symmetric set of S with respect to the origin, by $\tilde{S}$.

2 Robust Morphological Operators

2.1 The Binary Case

Our starting point is the classical definition of an opening by a symmetric set S (called a *structural element*): a pixel x belongs to the opening of a binary image X by the structural element S iff x belongs to at least *one* translation of S *totally* included in X.

A natural generalization is to weaken the total inclusion requirement to several partial ones, i.e., we require that x belongs to *at least* r_2 translations of S, which have *at least* r_1 pixels in common with the image X. The above can be formalized in the following way [9], [11].

Definition 1. *For a given structural element S, we define the morphological operator $R_S^{r_1,r_2}(\cdot)$ as:*

$$R_S^{r_1,r_2}(X) = \rho_{r_2,\tilde{S}}(\rho_{r_1,S}(X)), \tag{1}$$

where $\rho_{r,S}(\cdot)$ denotes the $r-$rank operator [1]*:*

$$\rho_{r,S}(X) = \{x : |S_{(x)} \cap X| \geq r\}. \tag{2}$$

One observes that $R_S^{1,|S|}(\cdot)$, $R_S^{|S|,1}(\cdot)$, $R_S^{|S|,|S|}(\cdot)$ and $R_S^{1,1}(\cdot)$ correspond respectively to a closing $(X \bullet S)$, opening $(X \circ S)$, a double erosion and dilation.

2.2 The General Case

One way to extend Def. 1 for binary images to gray scale images is through the use of the set of *slices* $X^{-1}(u) = \{x,\ X_x \geq u\}$.

Definition 2. *If X is a gray scale image and S a subset of pixels, we define the morphological operator $R_S^{r_1,r_2}(\cdot)$ as:*

$$R_S^{r_1,r_2}(X)_x = \max\{u : x \in \rho_{r_2,\tilde{S}}(\rho_{r_1,S}(X^{-1}(u)))\}. \tag{3}$$

Using the geometric interpretation of the operator for the binary case, one obtains:

Proposition 1. *The value of $R_S^{r_1,r_2}(X)$ at x corresponds to the largest possible value u such that x is contained in at least r_2 translations of S, that have at least r_1 pixels in common with $X^{-1}(u)$.*

[1] Also known in the literature as order statistic filter, percentile filter or Ξ filter.

2.3 Motivation

A motivation to introduce the above class of operators was given in [11]. As the result of $X \circ S$ and $X \bullet S$ is a basic step in the calculation of the *Pattern Spectrum* and is used in many composed operators like *Top-hats*, it is important to have at one's disposal a good estimator for $X \circ S$ and $X \bullet S$, when only $N(X)$, a noisy version of X, is available.

In [11] it was shown that if $N(X)$ is the result of limited ($< 5\%$) pepper and salt noise distortion on X, $R_S^{r_1,r_2}(N(X))$ is a robust approximation for $X \circ S$ and $X \bullet S$ (using appropriate values of r_1 and r_2).

The above should be contrasted with the construction of the *Rank-Max filters* [5] or, equivalently, *Regulated Openings* [1], where one embeds the classical morphological openings in a larger (parametrized) family, conserving the properties of an algebraic opening. Although less sensitive to noise than the morphological openings, several experiments showed that $R_S^{r_1,r_2}(\cdot)$ outperforms them.

Of course, a drawback is the absence of the idempotency property. In the next section, we study the limit behaviour under repeated applications. To this end, we define for any value of r_1 and r_2:

$$T^1(X) = R_S^{r_1,r_2}(X), \quad T^t(X) = R_S^{r_1,r_2}(T^{t-1}(X)).$$

3 Limiting Behaviour

3.1 The Binary Case

Proposition 2. *For any X, $T^t(X)$ will converge to a fixed image when t tends to infinity.*

Proof. It is illustrative to describe the dynamical behaviour of $T^t(X)$ by means of a cellular automaton. To this purpose, consider an image X of size $n \times m$ as one long vector of size nm with elements belonging to $\{0, 1\}$. We define the state space of the automaton as a vector Y^t with two components, $Y = (Y_1^t, Y_2^t)$, each of size nm. The dynamics of Y^t is described by:

$$Y^t = (\rho_{r_2,\tilde{S}}(Y_2^{t-1}), \rho_{r_1,S}(Y_1^{t-1})) \quad Y^0 = (X, X) \text{ with } X \text{ a given image.} \tag{4}$$

Consequently, Y_1^{2t} corresponds to $T^t(X)$, the application of t times $R_S^{r_1,r_2}(\cdot)$. We construct:

$$M_S = \begin{pmatrix} 0 & N_{\tilde{S}} \\ N_S & 0 \end{pmatrix} \tag{5}$$

where N_S is the $nm \times nm$ matrix:

$$(N_S)_{x,y} = \begin{cases} 1 \text{ if } y \in S_{(x)} \\ 0 \text{ otherwise.} \end{cases}$$

As $y \in S_{(x)}$ iff $x \in \tilde{S}_{(y)}$, M_S is a symmetric matrix. Next, define the vector $\theta = (r_2, \cdots, r_2, r_1, \cdots, r_1)$ where r_1 and r_2 are repeated nm times.

All together, because of (4), one obtains:

$$Y^t = \mathbb{1}(M_S Y^{t-1} - \theta), \tag{6}$$

where $\mathbb{1}(\cdot)$ is the vectorized threshold function (i.e. $(y_1, \cdots, y_n) = \mathbb{1}((x_1, \cdots, x_n))$ iff $y_i = I(x_i \geq 0)$ and $I(\cdot)$ denotes the Indicator function).

As there are only a finite number of elements in our state space, we can always find a θ_2 in such a way that:

$$M_S Y^{t-1} - \theta \geq 0 \text{ iff } M_S Y^{t-1} - \theta_2 > 0$$

and

$$M_S Y^{t-1} - \theta < 0 \text{ iff } M_S Y^{t-1} - \theta_2 < 0.$$

In the sequel we suppose that $\theta = \theta_2$ to guarantee that:

$$M_S Y^{t-1} - \theta \neq 0. \tag{7}$$

Following the derivation in [2] - which for the sake of completeness we include here - a Liapunov function is introduced, associating an energy with every state Y:

$$E(Y^t) = -\langle Y^t, M_S \cdot Y^{t-1} \rangle + \langle \theta, Y^t + Y^{t-1} \rangle,$$

where $\langle ., . \rangle$ denotes the usual inner product.
Using the fact that M_S is a symmetric matrix,

$$\Delta E := E(Y^t) - E(Y^{t-1}) = -\sum_x \{(Y_x^t - Y_x^{t-2})(\sum_y (M_S)_{x,y} Y_y^{t-1} - \theta_x)\}. \tag{8}$$

By construction each term in the outer sum in (8) is positive, hence ΔE is always non-positive. As the state space is finite, from a certain moment on, E remains constant[2]. Using once more that each term in the outer sum in (8) is positive, together with (7), $\Delta E = 0$ implies that there exists a given t_0, such that for $t > t_0$:

$$Y^{2t} = Y^{2t_0},$$

i.e., one obtains convergence of $T^t(\cdot)$ to a fixed image. □

As an illustration, in Fig. 1 the fixed points are shown under repeated application of $R_S^{r_1,r_2}(\cdot)$ for different parameter values.

The following property describes the fixed points (images) in the particular case where S equals a discrete circle of radius 1 in the city-block metric.

Proposition 3. *If S is a circle of radius 1 in the city-block metric,*

1. *the limit points of $R_S^{2,3}(\cdot)$ are of the form $\cup_l R_l$, where R_l are rectangles with a minimum (Euclidean) distance of $\sqrt{2}$ between them, i.e.:*

$$min_{r_k \in R_k, r_l \in R_l} d(r_k, r_l) \geq \sqrt{2}, \textit{ for } l \neq k; \tag{9}$$

2. the limit points of $R_S^{2,2}(\cdot)$ are of the form $\cup_l R_l$, where R_l are rectangles with a minimum (Euclidean) distance of two between them, i.e.:

$$min_{r_k \in R_k, r_l \in R_l} d(r_k, r_l) \geq 2, \text{ for } l \neq k.$$

Proof.
1. It is sufficient to show that the configurations of 2×2 pixels, shown in Fig. 2(a), can not form part of a fixed point(image). These configurations represent the only possible situations that can not be written as the union of rectangles satisfying (9).

Suppose the opposite holds; independent of the values of the neighbouring points, the application of $R_S^{2,3}(\cdot)$ to any of the configurations of Fig.2(a), will give rise to the configuration shown in Fig.2(b) causing a contradiction with the fact that Fig. 2(a) forms part of a limiting point.

In Fig. 3 a limit point is shown that illustrates that the lower bound of the distance between the rectangles can be attained.

2. In this case, we obtain a classical 2−threshold cellular automaton for which Prop. 4.5 of [2] can be applied.

□

3.2 The General Case

In order to extend Prop. 2. to gray scale images, we make use of the concept of an *umbra*, defined as [8]:

$$Um(X) = \{(x, u) : u \leq X_x\}. \tag{10}$$

If we abbreviate $\{(a, x),\ a \in A\}$ by (A, x) with A an arbitrary set, an umbra of an image is equivalent to:

$$Um(X) = \cup_u (X^{-1}(u), u). \tag{11}$$

We denote by $Um^{-1}(\cdot)$ the operator that maps $Um(X)$ into X.

Using the above, we can associate with any order preserving set function $f(\cdot)$ (i.e., $A \subset B$ implies $f(A) \subset f(B)$) an operator $\mathcal{F}(\cdot)$ on X in the following way:

$$\mathcal{F}(X) = Um^{-1}(\cup_u (f(X^{-1}(u)), u)).$$

The following lemma shows how the result of a composition of certain functions acting on an image, is related to the calculation of a composition of corresponding functions acting on each slice of the image.

Lemma 1. *Suppose that $f(\cdot)$ and $g(\cdot)$ are two order preserving set functions. If we define $\mathcal{F}(\cdot)$ and $\mathcal{G}(\cdot)$ by:*

$$\mathcal{F}(X) = Um^{-1}(\cup_u (f(X^{-1}(u)), u)), \ \ \mathcal{G}(X) = Um^{-1}(\cup_u (g(X^{-1}(u)), u)),$$

then

$$\mathcal{F}(\mathcal{G}(X)) = Um^{-1}(\cup_u (f(g(X^{-1}(u))), u)).$$

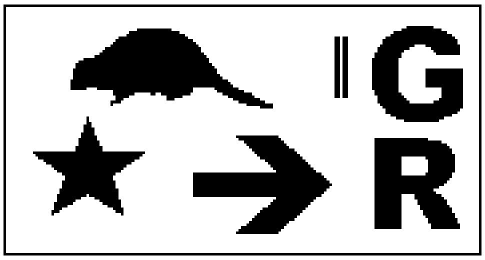

(a)

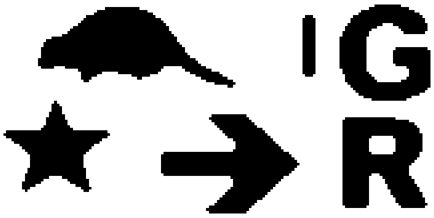

(b)

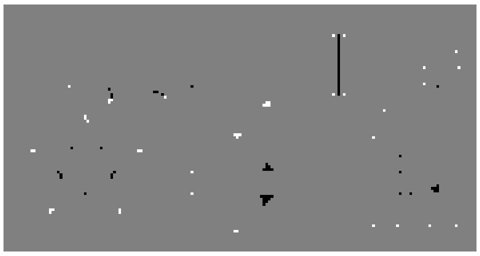

(c)

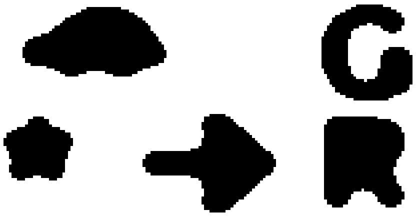

(d)

(e)

Fig. 1. (a): the given image X; (b): limit of $R^{2,4}_{S_1}(X)$; (c): limit of $R^{2,4}_{S_1}(X) - X$ (black denotes a positive difference, white a negative one); (d): limit of $R^{4,10}_{S_2}(X)$; (e): limit of $R^{2,3}_{S_1}(X)$ and S_1, S_2 denotes a circle of radius 1 resp. 2.

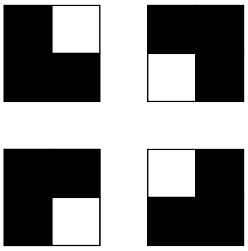

(a)

(b)

Fig. 2.

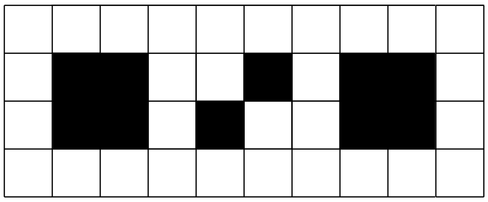

Fig. 3. A limit point of $R_S^{2,3}(\cdot)$, composed of four rectangles, the two in the middle are separated by a distance of $\sqrt{2}$.

Proposition 4. *For any structural element, S, repeated applications of $R_S^{r_1,r_2}(\cdot)$ will converge to a fixed image.*

Proof. If $f(\cdot)$ is an order preserving set function and Z a gray scale image, we have the following equivalence, which is easy to demonstrate:

$$Um(Z) = \cup_u(f(X^{-1}(u)), u) \;\text{ iff }\; \forall x : Z_x = \max\{u : x \in f(X^{-1}(u))\}. \tag{12}$$

Hence, Def. 2 is equivalent to:

$$Um(R_S^{r_1,r_2}(X)) = \cup_u(\rho_{r_2,\tilde{S}}(\rho_{r_1,S}(X^{-1}(u))), u). \tag{13}$$

Using Lemma 1., if we choose $f(\cdot) = g(\cdot) = R_S^{r_1,r_2}(\cdot)$, then repeated applications of $R_S^{r_1,r_2}(\cdot)$ is equivalent to repeatedly applying this operator to each slice and taking the union (or equivalent the supremum) at the end. For each slice, Prop. 2 guarantees convergence. □

An example is shown in Fig. 4 for different values of $R_S^{r_1,r_2}(\cdot)$. As one observes in Fig. 4(d), the limit point is not sensitive to the presence of low salt and pepper noise in the original image.

Although for all the above examples convergence was reached in less than ten iterations, a considerable speed-up (25%) of the calculation time was obtained using a *moving-histogram* algorithm to calculate $\rho_{r,S}(X)$, instead of its naive direct implementation. The basic idea of the *moving-histogram* algorithm [10] is to update the histogram of the gray values of the pixels covered while sliding the structural element over the image. This is usually a much smaller set than all pixel values, the update step is extremely efficient and the value of $\rho_{r,S}(X)$ can be easily obtained.

In the particular case of binary images, other alternatives are available. We refer to [12] for a recent overview.

4 Extensions to Soft Morphological Filters

The above construction is not only useful for the class of operators introduced in section 2. As an example, we consider the following class of soft morphological

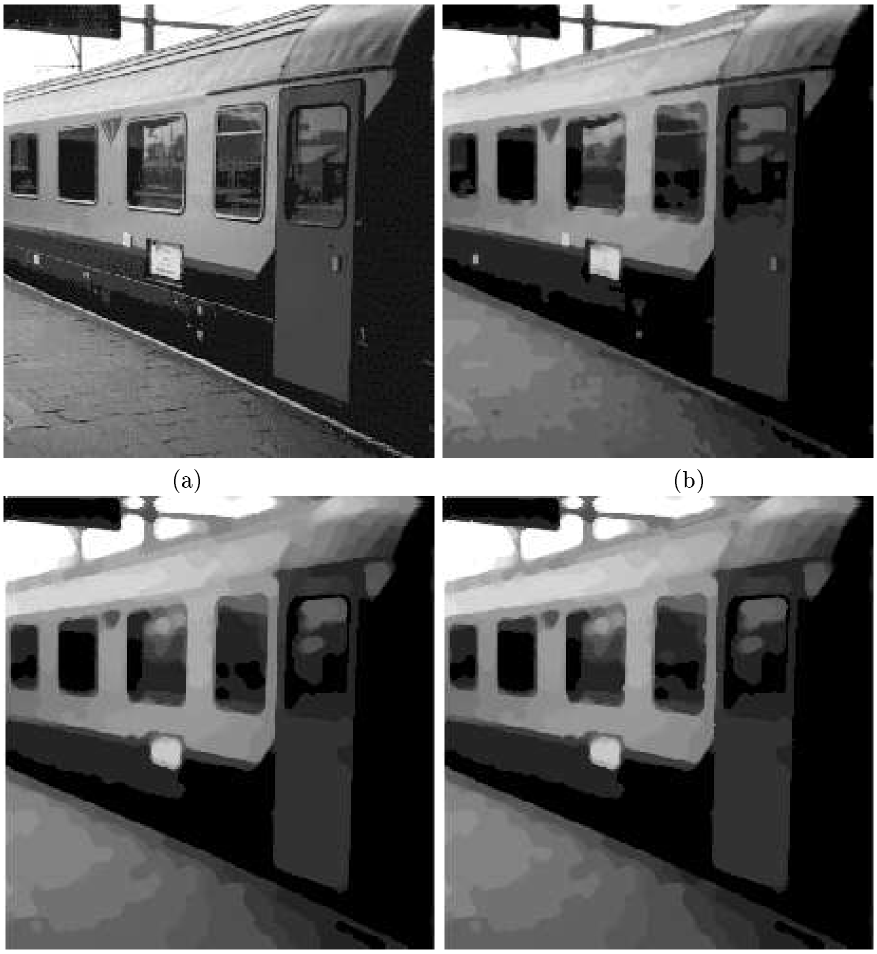

(a) (b) (c) (d)

Fig. 4. (a): the given image X; (b): limit of $R_{S_1}^{2,4}(X)$; (c): limit of $R_{S_2}^{3,7}(X)$; (d): limit of $R_{S_2}^{3,7}(N(X))$ where $N(X)$ denotes X corrupted by 1% salt and pepper noise and S_1, S_2 denote a circle of radius 1 resp. a 3×3 rectangle.

filters (several definitions appear in the literature; we follow the one of [4]). For the sake of simplicity, we restrict ourselves to soft morphological openings for binary images.

Definition 3. *[4] Given two symmetric sets $S^{\mathcal{H}}$, $S^{\mathcal{S}}$, $S^{\mathcal{H}} \subset S^{\mathcal{S}}$ and $r \leq |S^{\mathcal{S}} \setminus S^{\mathcal{H}}|$, define the soft morphological opening, $X \circ [S^{\mathcal{H}}, S^{\mathcal{S}}, r]$, as:*

$$X \circ [S^{\mathcal{H}}, S^{\mathcal{S}}, r] = (X \ominus [S^{\mathcal{H}}, S^{\mathcal{S}}, r]) \oplus [S^{\mathcal{H}}, S^{\mathcal{S}}, r], \tag{14}$$

where $(X \ominus [S^{\mathcal{H}}, S^{\mathcal{S}}, r])_x$, $(X \oplus [S^{\mathcal{H}}, S^{\mathcal{S}}, r])_x$ denote the rth smallest, respectively, rth largest value of the multiset[2] *$(r \diamond (S^{\mathcal{H}}_{(x)} \cap X)) \cup ((S^{\mathcal{S}} \setminus S^{\mathcal{H}})_{(x)} \cap X)$, and where $\diamond$ denotes de repetition operator ($r \diamond S$ equals r times the multiset S).*

In a similar way, a soft morphological closing is defined.

Proposition 5. *The repeated application of a soft morphological opening (closing) will converge to a fixed image.*

Proof. Only minor changes in the proof of Prop. 2 have to be done. The dynamics can be described by a dynamical system similar to (6). In (5), we should now define:

$$(N_S)_{x,y} = \begin{cases} r \text{ if } y \in S^{\mathcal{H}}_{(x)} \\ 1 \text{ if } y \in S^{\mathcal{S}}_{(x)} \setminus S^{\mathcal{H}}_{(x)} \\ 0 \text{ otherwise.} \end{cases}$$

As N_S is also symmetrical, the same reasoning of the proof of Prop. 2 applies and the same conclusions hold.

□

5 Conclusions

In this paper we have proven that the repeated application of a certain class of discrete image operators converge to a fixed image. Although only some modest but promising results concerning the characterization of those limiting points were included, a lot of work still has to be done.

Some open questions are: For which parameter values of r_1, r_2 do we obtain a union of convex sets as the limit image? When do we obtain a non-trivial limit (i.e., an image that is not completely black or white)? How do we obtain an tight upper and lower bound of this image? How do we obtain a good upper bound of the convergence speed?

Acknowledgement

The authors like to thank a referee and I. Terol for a variety of suggestions that helped in the revision of the paper.

[2] A multiset is a collection where repetition of the objects is allowed.

References

[1] Agam, G., Dinstein, I.: Regulated Morphological Operators. Pattern Recognition **32** (1999) 947–971

[2] Goles, E., Martínez, S.: Neural and Automata Networks: Dynamical Behavior and Applications. Kluwer Academic Publishers (1990)

[3] Heijmans, H.: Morphological Image Operators. Academic Press (1994)

[4] Koskinen, L., Astola, J., Neuvo, Y.: Soft Morphological Filters. SPIE Image Algebra and Morphological Image Processing II (1991) 262–270

[5] Ronse, C.: Erosion of Narrow Image Features by Combination of Local Low Rank and Max Filters. Proceedings 2nd Int. Conf. on Image Processing and its Applications, London, (1986) 77–81

[6] Serra, J.: Image Analysis and Mathematical Morphology, Volume I. Academic Press (1982)

[7] Soille, P.: Morphological Image Analysis : Principles and Applications. Springer Verlag (1999)

[8] Sternberg, S.R.: Parallel Architecture for Image Processing. In Proc. Third International IEEE Compsac, Chicago (1979)

[9] Tapia-Rodriguez, E.: A Study of Robust Mathematical Morphology for the Analysis of Discrete Images (in spanish). Master Thesis, CIMAT (1998)

[10] Van Droogenbroeck, M., Talbot, H.: Fast Computation of Morphological Operations with Arbitrary Structuring Elements. Pattern Recognition Letters **17** (1996) 1451-1460

[11] Van Horebeek, J., Tapia-Rodriguez, E.: The Approximation of Openings and Closings in the Presence of Noise. Signal Processing (to appear)

[12] Zmuda, M., Tamburino, A.: Efficient Algorithms for the Soft Morphological Operators. IEEE-PAMI **18** (1996) 1142–1147